IEEE Access
Multidisciplinary ⋮ Rapid Review ⋮ Open Access Journal

Received 2 February 2023, accepted 15 February 2023, date of publication 22 February 2023, date of current version 27 February 2023.

Digital Object Identifier 10.1109/ACCESS.2023.3247342

RESEARCH ARTICLE

Beamspace Selection in Multi-User Massive MIMO

VLADISLAV MOLODTSOV, ROMAN BYCHKOV, ALEXANDER OSINSKY, DMITRY YAROTSKY, AND ANDREY IVANOV

Skolkovo Institute of Science and Technology, 121205 Moscow, Russia

Corresponding author: Andrey Ivanov (an.ivanov@skoltech.ru)

The research was carried out at Skoltech and supported by the Russian Science Foundation (project no. 21-11-00373).

ABSTRACT In this paper, we propose new Discrete Fourier Transform (DFT)-based beamspace selection algorithms for Massive Multiple Input, Multiple Output (MIMO) receiver operating in realistic multi-user (MU) scenarios. In practical uplink scenarios, there is a power ratio between signals received from different users that complicates performance analysis in MU cases. Our algorithms are inspired by a proportional fair approach to allocating spatial resources for target users. Thus, we analyze performance in terms of coverage (for low-power users) and capacity (for high-power users) and consider the implementation complexity to highlight feasible algorithms. Simulations with realistic non-line-of-sight scenarios generated by the QuaDRiGa 2.0 demonstrate our methods outperform other DFT-based alternatives, such as the beamspace selection based on the projection power maximization.

INDEX TERMS 5G, multi-user massive MIMO, beamspace selection, angular domain processing.

I. INTRODUCTION

The rapid increase in the amount of mobile traffic and the emergence of new scenarios such as the Internet of Things (IoT) and Machine-to-Machine communication (M2M) require the development of the next, fifth-generation (5G) of wireless technologies [1]. Thus, modern 5G networks are subject to extraordinarily strict requirements. For instance, they should provide data rates up to 10Gbps, which is orders of magnitude improvement over 4G networks, or extremely low latency of 1 millisecond, compared to 200 milliseconds in 4G [2].

One of the most promising technologies [3] to meet the demand for high data throughput and spectral efficiency in 5G is Massive Multiple Input Multiple Output (MIMO), a concept when the number of antennas at the Base Station (BS) is much larger than the number of antennas at the User Equipment (UE) [4]. One of the key features of Massive MIMO is that it efficiently leverages Multi-User (MU) transmissions [5] which allows it to simultaneously serve several UEs in the same resource blocks. Thereby, MU Massive MIMO can lead to significantly increased system throughput and spectral efficiency and help to meet the requirements of 5G [6].

The main problem preventing 5G Massive MIMO from being ubiquitous is the huge computational complexity compared to classical (e.g. 4G) MIMO systems [7]. The number of antennas in 5G Massive MIMO is at least an order of magnitude larger than the number of antennas in 4G MIMO. Therefore, both Channel Estimation (CE) and MIMO detection require two orders of magnitude more computational resources. In addition, increased complexity induces additional overhead caused by data transportation from the Remote Radio Head (RRH) via a Common Public Radio Interface (CPRI) to the Base Band Unit (BBU) where CE and MIMO detection are implemented [8] as shown in Figure 1.

The high complexity of the Massive MIMO has attracted a lot of researchers recently, and a range of complexity reduction approaches based on channel sparsity has been proposed over the past few years [9]. The main idea of such techniques is based on the fact that a typical wireless multipath channel consists of only a finite number of scatterers corresponding to different propagation paths [10]. In Massive MIMO, the number of antennas is much higher than the number of scatterers in the environment, therefore, the channel tends to have an exceptionally sparse structure [11].

The associate editor coordinating the review of this manuscript and approving it for publication was Walid Al-Hussaibi.

To find this structure, the authors of the paper [12] explicitly built the estimated channel matrix by finding Directions of Arrival (DoA) for each user using some DoA estimation algorithm [13], while the authors of the paper [14] proposed a compressive sensing-based low-rank approximation of the channel matrix to translate the CE problem to a quadratic semidefinite programming problem that can be solved more efficiently. Another approach utilizes the sparsity of the channel covariance matrix to reduce the number of effective channel dimensions [15], [16].

More complexity reduction approaches come from the antenna array theory [17]. It is possible to perform CE and MIMO detection in another spatial domain having less dimensionality [18] as shown in Figure 1 for the MU case. The problem can be reformulated as finding a transformation to a modified spatial domain called beamspace [7] or angular domain [19] where the channel matrix and the received signal vector have only a few non-zero elements, while most others are zeros or close to zero. Therefore, one can consider a low dimensional domain to transform signals there with almost no loss of information [19].

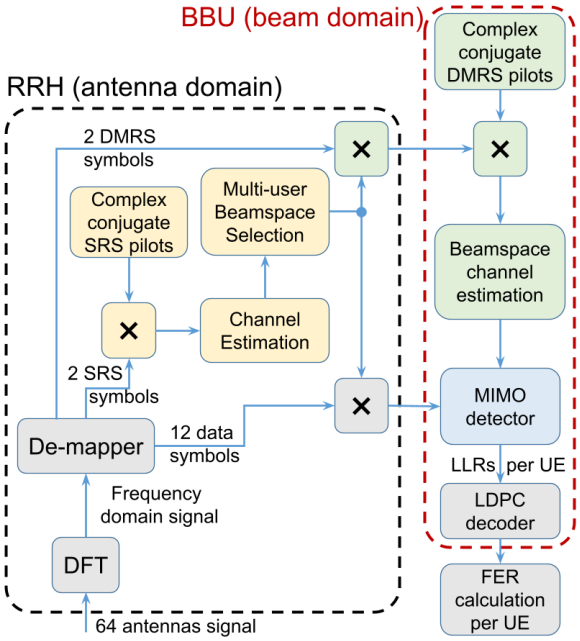

FIGURE 1. Receiver structure.

A. RELATED WORK

A lot of work in the area of beamspace selection has been done for Single-User (SU) Massive MIMO [7], [18], [20], [21], [22]. Paper [18] proposed to use Discrete Fourier transform (DFT) for angular domain transformation since it can be efficiently implemented using Fast Fourier transform (FFT). Papers [20], and [21] have found additional tricks to make selected beams more likely to capture dominant propagation paths by introducing multiple DFT matrices and performing additional rotation of the DFT basis, respectively. Paper [22] used DFT to perform initial dimensionality reduction as in paper [18] followed by Singular Value Decomposition (SVD) to construct the desired low dimensional basis. Finally, in [7] authors chose beamspace transformation according to the channel tap distribution found both offline and online in order to improve angular domain selection.

However, the problem of beamspace selection in the case of MU transmissions (MU BeamSpace Selection – MBSS) has not yet been studied enough. Existing works have only considered simplified cases when all users had the same channel conditions [19], [23], [24], [25], [26], [27], [28], [29], [30]. For example, in papers [19], [23], and [24], the authors have used data measured via real Massive MIMO testbed [31], [32], but the channel matrix for each UE has been normalized to remove the imbalance in attenuation between users, while in papers [25], [26], [27], [28], [29], and [30], channels for all UEs have been sampled from the same distribution.

Moreover, the authors have considered all users together trying to maximize total throughput [25], [27], [28], [30] and spectral efficiency [26], [29] or minimize average Bit/Block/Frame Error Rate (BER, BLER, FER, respectively) [19], [23], [24], [33]. At the same time, it has not been analyzed how a certain algorithm affects throughput or BER for each particular UE. An outstanding exception is a paper [33] where the authors used the geometric one-ring model and dropped UE devices randomly around the BS. Such a way of generating channels allowed them to simulate power imbalance. However, they still measured average BER among all users and did not consider the degradation of *weak* users.

Joint processing of users is a common approach for evaluating MIMO performance, not only in the case of MBSS but in MU MIMO in general. For instance, papers [34], and [35] have studied user pairing in uplink MIMO and measured the dependency of average BLER on Signal-to-Noise Ratio (SNR) in different cases. All UEs have been considered together, and the channels for them have been sampled from the same distribution. In the paper [36], the authors explicitly stated that all users had the same transmit signal power and path loss. Finally, the authors of the paper [37] presented an interference suppression detector for MU Massive MIMO and selected UEs with approximately the same power to test its performance.

The joint processing of users is justified by the criteria of grouping UEs with similar path losses, while different groups of users are time-multiplexed [32]. Another explanation is based on uplink power control, which should remove the imbalance in channel attenuation for different users [19]. However, in real scenarios, it is not always possible to pair users with almost the same received power or to properly control their transmission power [38]. In addition, according to the paper [34], other scheduling approaches that do not necessarily pair users with similar attenuation are sometimes beneficial, for instance, random pairing, the simplest from a practical point of view, or maximum-

minimum pairing and offset pairing which consciously combines users with unequal power to assist Successive Interference Cancellation (SIC) receiver [39], [40], [41]. Thereby, the analysis of MU Massive MIMO performance should not be limited to only simple cases, when all users are in similar channel conditions, but should be also expanded to real cases with a large imbalance in channel attenuation among users.

Moreover, consideration of scenarios with significant differences in received signal power is even more important in the context of MBSS. For example, consider a case when two users have different received signal powers at the BS side. The commonly used approach of selecting beams corresponding to the highest power [23], [33] totally fails in this case, giving preference to the *strong* user while entirely depriving the *weak* one of almost all power in the beamspace. Therefore, for designing a proper MBSS algorithm, additional separate consideration of each user is required to find out how certain MBSS techniques affect *weak* UEs if there is a difference in the received power.

B. OUR CONTRIBUTION

In this paper, we fill the above-mentioned gap by proposing a new methodology for MBSS approach investigation in MU Massive MIMO. Instead of examining all users together by calculating the dependency of throughput or FER on SNR for all users together, we suggest inspecting these dependencies for each user separately and highlighting *strong* and *middle* users responsible for capacity and the *weak* ones responsible for coverage. We suggest new beamspace selection algorithms and, based on the proposed methodology, justify their advantages.

Thus, the contribution of this paper can be summarized as follows:

1) First, we analyze MBSS methods designed before, show their weaknesses and, based on that, propose new MBSS algorithms.
2) Second, we compare different MBSS algorithms in realistic scenarios with a random imbalance in the received power among users (the channel is generated by the simulator [42]) while investigating how both *strong* and *weak* users are affected.
3) Finally, based on experimental results and complexity analysis, we demonstrate that some of the DFT-based algorithms proposed in this paper perform better than other DFT-based beamspace selection algorithms.

The organization of the paper is as follows. In Section II, the MBSS problem is formulated. In Section III, we review existing MBSS techniques and propose new algorithms. In Section IV, the computational complexity of MBSS methods is analyzed. Section V demonstrates the suggested methodology for comparing MBSS algorithms, while Section V represents the results of simulations with the Quadriga 2.0 [42] channel generator for a 64-antenna BS. Finally, Section VII concludes the paper.

C. NOTATION

Bold capital letters and numbers below them denote matrices and their size, respectively, e.g.

$$\underset{M\times N}{\mathbf{A}} \in \mathbb{C}^{M\times N}$$

is an $M \times N$ matrix with complex values. Similarly, bold lowercase letters and numbers below them denote vectors and their size, e.g.

$$\underset{M\times 1}{\mathbf{a}} \in \mathbb{C}^{M\times 1}$$

is an $M \times 1$ column vector with complex values.

$\mathbf{A}^H$ and $\mathbf{a}^H$ are the Hermitian conjugates of the matrix $\mathbf{A}$ and the vector $\mathbf{a}$, respectively, $\overline{\mathbf{a}}$ is a complex conjugate of the vector $\mathbf{a}$. Matrix product of two matrices $\mathbf{A}$ and $\mathbf{B}$ with sizes $N \times M$ and $M \times K$ is denoted as $\mathbf{A} \times \mathbf{B}$, while the elementwise product of two vectors $\mathbf{a}$ and $\mathbf{b}$ with equal sizes is denoted as $\mathbf{a} \odot \mathbf{b}$.

$|\cdot|$ is the absolute value of the scalar, while $\|\cdot\|$ is the Euclidean vector norm: $\|\mathbf{a}\| = \sqrt{\sum_k |a_k|^2}$.

Concatenation of M vectors $\mathbf{a}_i \in \mathbb{C}^{N\times 1}$, $i \in \overline{1,\ M}$ is denoted as follows:

$$\left[\mathbf{a}_1\ \mathbf{a}_2\ \ldots\ \mathbf{a}_M\right] \in \mathbb{C}^{N\times M}.$$

Parentheses denote dependencies, e.g. $\mathbf{a}(k)$, $\mathbf{b}(t)$, or $\mathbf{c}(k,t)$, while the j-th element of the vector $\mathbf{a}$ is denoted by square brackets as $a[j]$. Expectation and variance of $a(x)$ over a random variable x are $\underset{x}{\mathbb{E}}\, a$ and $\underset{x}{\mathbb{V}}\, a$, respectively. The maximum element in the set $\{a_i | i \in \overline{1,N}\}$ is $\max\limits_{i\in\overline{1,N}} a_i$.

II. MBSS PROBLEM

A. CHANNEL MODEL

The received antenna signal at k-th subcarrier and time moment t is given by the equation:

$$\underset{N\times 1}{\mathbf{y}(k,t)} = \underset{N\times M}{\mathbf{H}(k,t)} \times \underset{M\times 1}{\mathbf{x}(k,t)} + \underset{N\times 1}{\mathbf{z}(k,t)}, \tag{1}$$

where $\mathbf{x}$ is the vector of signals transmitted by M users, $\mathbf{y}$ is the vector of signals received by N BS antennas, $\mathbf{H}$ is the matrix of the channel between UEs and BS, $\mathbf{z} \sim \mathcal{CN}(0, \frac{\sigma^2}{N}\mathbf{I})$ is the vector of Additive White Gaussian Noise (AWGN) with noise power per antenna $\frac{\sigma^2}{N}$. Total numbers of subcarriers and time symbols are K and T: $k \in \overline{1,K}$, $t \in \overline{1,T}$. Given that m-th column of $\mathbf{H}(k,t)$ is the vector $\mathbf{h}_m(k,t)$, one can define the power of m-th user as $P_{user}(m) = \underset{n,k,t}{\mathbb{E}} |\mathbf{h}_m[n](k,t)|^2$.

The problem of MIMO detection can be formulated as finding the vector $\mathbf{x}$ using the received vector $\mathbf{y}$ and estimated channel $\mathbf{H}$. In case of linear detection, estimate $\hat{\mathbf{x}}$ of the desired $\mathbf{x}$ can be obtained by the detector's matrix $\mathbf{G}$:

$$\underset{M\times 1}{\hat{\mathbf{x}}(k,t)} = \underset{M\times N}{\mathbf{G}(k,t)} \times \underset{N\times 1}{\mathbf{y}(k,t)}, \tag{2}$$

where matrix $\mathbf{G}$ can be calculated using the channel estimate obtained from the pilot signals [43], [44].

B. BEAMSPACE DIMENSIONALITY REDUCTION

Equation (1) is a channel model in the antenna domain, where the element $\mathbf{y}[j](k,t)$ is a signal received at the j-th antenna. The basic idea of beamspace dimensionality reduction is finding a transformation to another domain where the image $\mathbf{y}^b(k,t)$ of $\mathbf{y}(k,t)$ has a sparse structure. For simplicity, it is common to apply a linear transformation, which can be described by a square matrix $\mathbf{W}$:

$$\underset{N\times 1}{\mathbf{y}^b(k,t)} = \underset{N\times N}{\mathbf{W}} \times \underset{N\times 1}{\mathbf{y}(k,t)}. \tag{3}$$

Since $\mathbf{y}^b(k,t)$ is sparse, one can select L rows in matrix $\mathbf{W}$ corresponding to the non-zero elements in $\mathbf{y}^b(k,t)$ and compose matrix $\mathbf{F}$ with size $L \times N$. After transformation by matrix $\mathbf{F}$, the image $\tilde{\mathbf{y}}(k,t)$ of the vector $\mathbf{y}(k,t)$ will have lower dimensionality:

$$\underset{L\times 1}{\tilde{\mathbf{y}}(k,t)} = \underset{L\times N}{\mathbf{F}} \times \underset{N\times 1}{\mathbf{y}(k,t)}. \tag{4}$$

Let us note that the sparse structure of the modified signal allows for reduced dimensionality with minimal loss of signal power.

C. BEAMSPACE SELECTION

In 5G, special reference signals are utilized for CE allowing the use of an efficient scheduler, precoder, and detector [45]. One of the reference signals in uplink is the Sounding Reference Signal (SRS). The SRS is wideband and powerful, therefore, it appears to be applicable for finding the transformation matrix $\mathbf{F}$ as well [7].

Generally, SRS is employed to achieve an estimate $\hat{\mathbf{H}}(k)$ of the channel matrix $\mathbf{H}(k,t)$. The matrix $\hat{\mathbf{H}}(k)$ has size $N \times M$ and each column $\hat{\mathbf{h}}_m(k)$, $m \in \overline{1,M}$ corresponds to the estimated channel between m-th user and base station. Thus, the problem of MBSS can be formulated as finding the reduced transformation matrix $\mathbf{F}$ given estimated $\hat{\mathbf{h}}_m(k)$, $m \in \overline{1,M}$.

Note the DoA is invariant to the subcarrier index for a majority of user signals. Therefore, the matrix $\mathbf{F}$ does not depend on the subcarrier index k. Moreover, we assume that $\mathbf{F}$ does not depend on the time moment t, since DoA changes too slowly and can be assumed constant for the SRS transmission period, as will be further described in Section V-A.

After the matrix $\mathbf{F}$ is selected, all further signal processing such as MIMO detection can be done with the new signal $\tilde{\mathbf{y}}$ [46]. For that, we need to use the estimated channel $\hat{\mathbf{H}}(k)$ transformed to the beamspace domain via matrix $\mathbf{F}$ as in equation (4).

III. MBSS ALGORITHMS

In practice, it is impossible to find a transformation matrix $\mathbf{F}$ which significantly reduces dimensionality and, at the same time, does not lose signal power. Therefore, the common approach is to, first, define the dimensionality L of the reduced beamspace, and then select L beams maximizing some metrics. Thus, the choice of transformation is always a trade-off between complexity reduction and loss of SNR.

Moreover, the situation becomes significantly more complicated in the case of MU transmissions, since more degrees of freedom have to be employed. For instance, as discussed in Section I, it is not trivial to select beams or basis vectors for the beam domain in the case of two UEs with different signal powers. The first way is to give preference to the *strong* or *weak* user, while the second one is to somehow select beams having signal power for both users. Thus, in the MU case, there is a trade-off not only between complexity and total signal power but between complexity, total signal power, and fairness of power distribution among users.

In this section, we analyze existing beamspace selection algorithms for both SU and MU cases and indicate their weaknesses. Based on that, we propose new approaches designed to solve found issues. The idea of all considered methods is the same. First, find a full transformation matrix $\mathbf{W}$ which can transform the signal to the beamspace domain with minimal loss of power. Second, select L beams or rows of $\mathbf{W}$ and compose a reduced transformation matrix $\mathbf{F}$. All methods can be split into two groups depending on which algorithm is used to find $\mathbf{W}$: the first group is DFT-based, and the second one is SVD-based. Sections III-A and III-B are devoted to each of them, respectively.

A. DFT-BASED BEAMSPACE SELECTION

DFT can be efficiently implemented via Fast Fourier Transform (FFT), therefore, DFT-based methods for beamspace selection are the most popular. For example, they are used in papers [18], [19], [20], [21], [22], [23], [23], [24], [25], [26], [27], [28], [29], [30] and [33]. The main idea of DFT-based beamspace selection for both SU and MU cases is that the full transformation matrix $\mathbf{W}$ is a DFT matrix. The matrix $\mathbf{W}$ is then used to convert the estimated channel for m-th user $\hat{\mathbf{h}}_m(k)$, $m \in \overline{1,M}$ to beam domain:

$$\underset{N\times 1}{\hat{\mathbf{h}}^b_m(k)} = \underset{N\times N}{\mathbf{W}} \times \underset{N\times 1}{\hat{\mathbf{h}}_m(k)}. \tag{5}$$

In this section, we denote $\hat{\mathbf{h}}^b_m(k)$ as $\mathbf{h}_m(k)$ for clarity. Thus, in the case of MU transmission, the input for beamspace selection algorithms is $\mathbf{h}_m(k)$, $m \in \overline{1,M}$, while the output is a set of indices $\mathcal{B}$ such that rows of $\mathbf{W}$ with indices in $\mathcal{B}$ form matrix $\mathbf{F}$. The power of set $\mathcal{B}$ is equal to the dimensionality of the reduced beamspace: $|\mathcal{B}| = L$.

Further, we describe each of the considered MBSS algorithms in detail.

1) DFT NON-NORMALIZED SUM POWER MAXIMIZATION

selects a set of indices $\mathcal{B}$ corresponding to the L largest values in the vector $\mathbf{P}_{beam}$

$$P_{beam}[i] = \sum_{m=1}^{M} \sum_{k} |h_m[i](k)|^2, \tag{6}$$

thus maximizing the total power across all users, subcarriers, and beams.

Used as the main algorithm for MBSS in papers [23], and [33]. The drawback occurs in the case of users with different signal powers. In this case, the preference will be given to the *strong* one, while *weak* users will not be taken into account at all. Denoted as **DFT Non-norm sum pow** in subsequent sections.

2) DFT NORMALIZED SUM POWER MAXIMIZATION (PROPOSED)

selects a set of indices $\mathcal{B}$ corresponding to the L largest values in the vector $\check{\mathbf{P}}_{beam}$ maximizing the *normalized* total power across users, subcarriers, and beams.

$$\check{P}_{beam}[i] = \sum_{m=1}^{M} \sum_{k} \frac{|h_m[i](k)|^2}{P_{sum}(m)}, \tag{7}$$

where

$$P_{sum}(m) = \sum_{k} \mathbf{h}_m^H(k) \times \mathbf{h}_m(k) \tag{8}$$

is the total power of the m-th user across all subcarriers and beams. It avoids the drawback related to the imbalance in the case of users with different powers. Denoted as **DFT Norm sum pow** in subsequent sections.

3) DFT NORMALIZED MAX POWER MAXIMIZATION (PROPOSED)

selects a set of indices $\mathcal{B}$ corresponding to the L largest values in the vector $\mathbf{P}$ constructed in a *normalized* way:

$$P[i] = \max_{m \in \overline{1,M}} \sum_{k} \frac{|h_m[i](k)|^2}{P_{sum}(m)}, \tag{9}$$

where $P_{sum}(m)$ is defined by (8). It is similar to **Norm sum pow** since it also overcomes the problem caused by the power imbalance among users. Denoted as **DFT Norm max pow** in subsequent sections.

4) DFT SHANNON CAPACITY MAXIMIZATION

selects a set of indices $\mathcal{B}$ which maximizes the total Shannon capacity [47] across users and subcarriers:

$$\sum_{m=1}^{M} \sum_{k} \log\Big(1 + SNR_m(k)\Big), \tag{10}$$

where $SNR_m(k)$ is SNR for m-th user at k-th subcarrier:

$$SNR_m(k) = \frac{\sum\limits_{i \in \mathcal{B}} |h_m[i](k)|^2}{P_{noise}}. \tag{11}$$

Here, P_{noise} is the total noise power in the beams corresponding to indices in the set $\mathcal{B}$. Assuming that the noise is uniformly distributed across beams, $P_{noise} = \frac{L}{N}\sigma^2$. Approaches similar to that were adopted in papers [27], and [29]. Denoted as **DFT Shannon** in subsequent sections.

5) DFT VARIANCE MAXIMIZATION

selects a set of indices $\mathcal{B}$ corresponding to the L largest values in the vector $\mathbf{V}$ constructed in the following way [23]:

$$V[i] = \mathop{\mathbb{V}}_{m}(P_{beam}(m, i)), \tag{12}$$

where

$$P_{beam}(m, i) = \sum_{k} |h_m[i](k)|^2 \tag{13}$$

is the total power of the m-th user in i-th beam across all subcarriers. Authors assume, that selecting the beams having the highest power variance among users implies these beams include some *strong* users as well as relatively *weak* ones. This fact makes it possible to easily detect data streams corresponding to *strong* UEs without significant interference from *weak* ones. Denoted as **DFT Highest variance** in subsequent sections.

6) DFT HIGHEST NUMBER OF STRONG UE

selects a set of indices $\mathcal{B}$ corresponding to the L beams having the highest number of "strong" UEs. Here, the user is considered "strong" in the beam if its total power across all subcarriers in this beam is higher than the average power of the user across all beams and subcarriers. Given the notations defined before, m-th UE is "strong" in i-th beam if

$$\sum_{k} |h_m[i](k)|^2 > \frac{1}{N} \sum_{k} \sum_{i \in \mathcal{B}} |h_m[i](k)|^2 \tag{14}$$

Proposed and used in papers [19], and [24]. Denoted as **DFT Max # of strong UE** in subsequent sections.

7) DFT ROUND-ROBIN (PROPOSED)

iterates circularly over all users $m = 1, 2, \ldots, M, 1, 2, \ldots, M, 1, \ldots$ until L beams are selected; at each iteration, adds to the set $\mathcal{B}$ an index $\hat{i}$ corresponding to the beam giving the maximum power to the user m in the beamspace:

$$\hat{i} = \arg\max_{i \in \check{\mathcal{B}}/\mathcal{B}} \sum_{k} |h_m[i](k)|^2, \tag{15}$$

where $\check{\mathcal{B}} = \{1, \ldots, N\}$ is the set of all indices, therefore, one should consider only those indices which have not yet been included in the set $\mathcal{B}$ at each iteration.

Has no drawback related to the power imbalance between users since it is guaranteed that the beams giving power to the *weak* user will be added to the set $\mathcal{B}$ as well. Denoted as **DFT Round-robin** in subsequent sections.

B. SVD-BASED BEAMSPACE SELECTION

SVD is more computationally heavy compared to FFT. However, it allows us to increase signal sparseness in the angular domain [22] thanks to a better alignment to propagation channel taps.

The main idea of the SVD-based beamspace selection is that the full transformation matrix $\mathbf{V}$ is obtained from SVD:

$$\underset{N \times M^*}{\mathbf{C}} = \underset{N \times N}{\mathbf{V}^H} \times \underset{N \times M^*}{\mathbf{S}} \times \underset{M^* \times M^*}{\mathbf{U}}, \tag{16}$$

where $M^* = M \times K$. Reduced transformation matrix $\mathbf{F}$ can be easily built of the first K rows of $\mathbf{V}$ since they correspond to the largest singular values and describe the angular domain most effectively.

One of the problems is how to construct matrix $\mathbf{C}$ providing an appropriate transformation matrix $\mathbf{F}$ after SVD. In this sense, we propose two ideas for building such a matrix $\mathbf{C}$ and discuss possible drawbacks. For convenience, let us introduce matrices $\mathbf{K}_m$, $m \in \overline{1, M}$, with size $N \times K$ such that their k-th column is equal to the estimated channel $\hat{\mathbf{h}}_m(k)$ in the antenna domain.

1) SVD NON-NORMALIZED

Desired matrix $\mathbf{C}$ is composed as a concatenation of matrices $\mathbf{K}_m$, $m \in \overline{1, M}$:

$$\underset{N\times M^*}{\mathbf{C}} = \Big[\underset{N\times K}{\mathbf{K}_1}\ \underset{N\times K}{\mathbf{K}_2}\ \dots\ \underset{N\times K}{\mathbf{K}_M}\Big]. \tag{17}$$

A similar approach is proposed in the paper [22]. A possible drawback is unfair beamspace selection in case of power imbalance among users, as discussed before. Denoted as **SVD Non-norm** in subsequent sections.

2) SVD NORMALIZED (PROPOSED)

Desired matrix $\mathbf{C}$ is composed as a concatenation of matrices $\mathbf{K}_m$, $m \in \overline{1, M}$ taking into account power imbalance:

$$\underset{N\times M^*}{\mathbf{C}} = \Big[\underset{N\times K}{\mathbf{K}_1^*}\ \underset{N\times K}{\mathbf{K}_2^*}\ \dots\ \underset{N\times K}{\mathbf{K}_M^*}\Big], \tag{18}$$

where $\mathbf{K}_m^* = \mathbf{K}_m / P_{user}(m)$, $m \in \overline{1, M}$, are *normalized* matrices, $P_{user}(m)$ is the power of m-th user as described in Section II-A.

This version of the SVD is insensitive to the power imbalance of users. Denoted as **SVD Norm** in subsequent sections.

IV. COMPUTATIONAL COMPLEXITY

In this section, the computational complexity of existing and proposed MBSS algorithms is analyzed. For operation in the beamspace domain, two steps are required. First, based on the received SRS, it is necessary to find the transformation matrix $\mathbf{F}$. Second, the antenna domain signal for T subsequent orthogonal frequency-division multiplexing (OFDM) symbols should be transformed to the beamspace using the selected transformation matrix. Here, T is the SRS period divided by the OFDM symbol duration, therefore, transformation to the beamspace is T times more frequent compared to the calculation of the transformation matrix. In practice, one should calculate the beamspace transformation matrix $\mathbf{F}$ faster than the whole SRS period as in fast-fading channels the DoA aging effect could appear, but for simplicity, we assume the full SRS period for the beamspace selection. Below is the detailed derivation of complexity for each MBSS method, while the total complexity for all algorithms is summarized in Table 1.

First, consider the complexity of the beamspace transformation. For DFT-based approaches, low-cost FFT can be utilized, leading to $\mathcal{O}(N \log N)$ operations [48] per each subcarrier of an OFDM symbol. For SVD-based approaches, instead of $\mathcal{O}(N \log N)$, full matrix multiplication with asymptotic $\mathcal{O}(NL)$ should be performed. Given M users, K subcarriers, and T OFDM symbols, the resulting complexity of the beamspace transformation for one SRS period is $\mathcal{O}(TMKN \log N)$ for DFT-based methods and $\mathcal{O}(TMKNL)$ for SVD-based ones.

Second, consider the complexity of transformation matrix selection. We assume that such selection is performed by SRS spanning to K subcarriers for each of M users. For **DFT Non-norm sum pow**, the total power over M users and K subcarriers for each of N beams can be calculated using equation (6), resulting in $\mathcal{O}(MKN)$ number of operations. Since the only difference between **DFT Non-norm sum pow** and **DFT Norm sum pow** is the division by (8) the **DFT Norm sum pow** method has extra $\mathcal{O}(MKN)$ complexity. **DFT Norm max pow** has the same complexity as **DFT Norm sum pow** since $\sum$ operation in (7) is just substituted with max in (9).

For **DFT Highest variance**, the power over K subcarriers is calculated for each of N beams and M users according to equation (13) that results in $\mathcal{O}(MKN)$ number of operations. Variance calculation over M users for N beams has $\mathcal{O}(MN)$ complexity, which is low.

For **DFT Max # of strong UE**, the powers from equation (13) should be obtained with $\mathcal{O}(MKN)$ complexity. Then, the average power among beams and the number of strong UE are computed requiring small $\mathcal{O}(MN)$ numbers of operations each.

Note that in the presented analysis of beamspace selection methods, we neglect the overhead of selecting the best L beams since it can be done only once for all subcarriers and users and requires only $\mathcal{O}(N \log L)$ operations.

To find the transformation matrix in **DFT Shannon**, we iteratively choose beams that provide the largest capacity in a greedy manner. At i-th iteration, $i = \overline{1, L}$, we check $N - i$ remaining beams that results in $L\frac{2N-L+1}{2}$ capacity calculations. To update the capacity estimation for a particular beam only $\mathcal{O}(MK)$ operations are needed. Thus, the resulting complexity is $\mathcal{O}(MKL\frac{2N-L}{2})$.

In the case of **DFT Round-robin**, the same number of iterations over beams is required: $L\frac{2N-L+1}{2}$. However, only $\mathcal{O}(K)$ operations are needed to compute the beam's contribution since we are interested in the power of one particular UE at each iteration. Moreover, after M chosen beams and $M\frac{2N-M+1}{2}$ iterations, all necessary contributions (13) are calculated, and the remaining steps become cheap. Therefore, the complexity is $\mathcal{O}(KM\frac{2N-M}{2})$.

Finally, in **SVD Non-norm**, SVD of the matrix with sizes $N \times KM$ should be calculated resulting in $\mathcal{O}(MKN^2)$ complexity [22] for transformation matrix selection, while in

TABLE 1. Computational complexity of MBSS algorithms.

Algorithm	Beamspace selection	Antenna to Beamspace transformation
DFT Non-norm sum pow [23, 33]	$\mathcal{O}(MKN)$	$\mathcal{O}(TMKN \log N)$
DFT Norm sum pow (proposed)	$\mathcal{O}(2MKN)$	$\mathcal{O}(TMKN \log N)$
DFT Norm max pow (proposed)	$\mathcal{O}(2MKN)$	$\mathcal{O}(TMKN \log N)$
DFT Shannon [27, 29]	$\mathcal{O}(MKL\frac{2N-L}{2})$	$\mathcal{O}(TMKN \log N)$
DFT Highest variance [23]	$\mathcal{O}(MKN)$	$\mathcal{O}(MKN \log N)$
DFT Max # of strong UE [19, 24]	$\mathcal{O}(MKN)$	$\mathcal{O}(TMKN \log N)$
DFT Round-robin (proposed)	$\mathcal{O}(KM\frac{2N-M}{2})$	$\mathcal{O}(MKN \log N)$
SVD Non-norm [22]	$\mathcal{O}(MKN^2)$	$\mathcal{O}(TMKNL)$
SVD Norm (proposed)	$\mathcal{O}(MKN^2 + MKN)$	$\mathcal{O}(TMKNL)$

case of **SVD Norm**, extra $\mathcal{O}(MKN)$ operations are spent for normalization as discussed before.

V. SIMULATION SCENARIOS

In this section, we discuss the experiments with the presented approaches. First, in Section V-A, a detailed description of the simulation is provided. Second, in Section V-B, we describe and justify the methodology used to compare MBSS algorithms.

A. SCENARIOS DESCRIPTION

The presented MBSS approaches were tested in realistic 5G simulations in numerous non-line-of-sight scenarios generated by the QuaDRiGa 2.0 channel [42]. For simulations, we utilized parameters described in Table 2 with the number of users M equal to 8 and 4. Massive MIMO receiver had 4 antennas in the vertical plane, 8 the in horizontal one, and 2 polarizations [49].

The simulation workflow is shown in Figure 1 and is close to a real Massive MIMO receiver. First, SRS signals are used to get a wideband estimation of the channel between UEs and BS. In our experiments, SRS occupied 2 OFDM symbols and 16 resource blocks, 12 subcarriers each, therefore, $K = 16 \times 12 = 192$. 1 Transmission Time Interval (TTI) was 0.5ms and contained 14 OFDM symbols, while the SRS transmission period was equal to 100 TTI.

Assume all users transmitted pilots orthogonally to avoid CE degradation. Thus, the approach proposed in the paper [50] was employed for CE. This method iteratively searches for propagation channel taps. Then, it denoises and spatially filters them taking into account antenna array configuration.

Note, that in a common CE using the beamspace processing [20], there is an optimal number of beams to save while all others are discarded. For example, if some beams contain much more noise than the useful signal, it is better to remove such beams in advance. However, in a recently proposed approach [50], such "noisy" beams are still useful since they can be denoised and utilized for finding minor DoA. Thus, there is a trade-off between performance and computational complexity: the fewer beams are discarded, the better CE is. The scenario when no beams are discarded corresponds to the lower bound of achievable FER. This case is equivalent to CE and MIMO detection in the antenna domain without any transformations to the beamspace. Such a case is called **Antenna domain** in subsequent sections.

The channel estimated by SRS was further used to find the proper beamspace transformation matrix $\mathbf{F}$ using one of the algorithms given in Section III as stated in Section II-C. Note that CE obtained with SRS once is used for the whole SRS transmission period. All algorithms from Section III selected $L = 16$ beams, thus, the dimensionality was reduced by a factor of 4: from 64 to 16.

TABLE 2. Simulation parameters.

Parameter	Value	Parameter	Value
Carrier frequency	3.5GHz	**Modulation**	QAM-16
Subcarrier spacing	30kHz	**N of scenarios**	140
BS height	25m	**N of noise seeds**	16
UE height	1.5m	**Decoder**	LDPC (144,288)
Vertical antennas spacing	0.9λ	**Channel model**	3GPP-3D, Berlin, Dresden
Horizontal antennas spacing	0.5λ	**Channel type**	NLOS
N of BS antennas	64	**UE speed**	5 km/h
N of UE antennas	2	**Distance to UE**	50...250m

After that, 100 TTIs are transformed to the beamspace domain using matrix $\mathbf{F}$. Note, 14 OFDM symbols (1 TTI) occupied 4 resource blocks of size 12 subcarriers. The narrowband signals contain 12 data symbols as well as 2 pilot symbols used for demodulation (DMRS) as indicated in Figure 1. Both data and pilot symbols were transformed to beamspace using the transformation matrix $\mathbf{F}$ found previously.

The found DMRS pilots were used for constructing the detector matrix $\mathbf{G}$, introduced in Section II-A. In simulations, we used Minimum Mean Square Error (MMSE) linear detector [51]. After calculating detected symbols $\hat{\mathbf{x}}$, they were demodulated and decoded. Finally, FER for each user was calculated as a performance metric for the given SNR.

B. METHODOLOGY OF COMPARISON

Let us note that existing works have only considered simplified cases when all users have the same channel conditions. In addition, all users have usually been analyzed together by measuring the average FER. Such an assumption leads to the

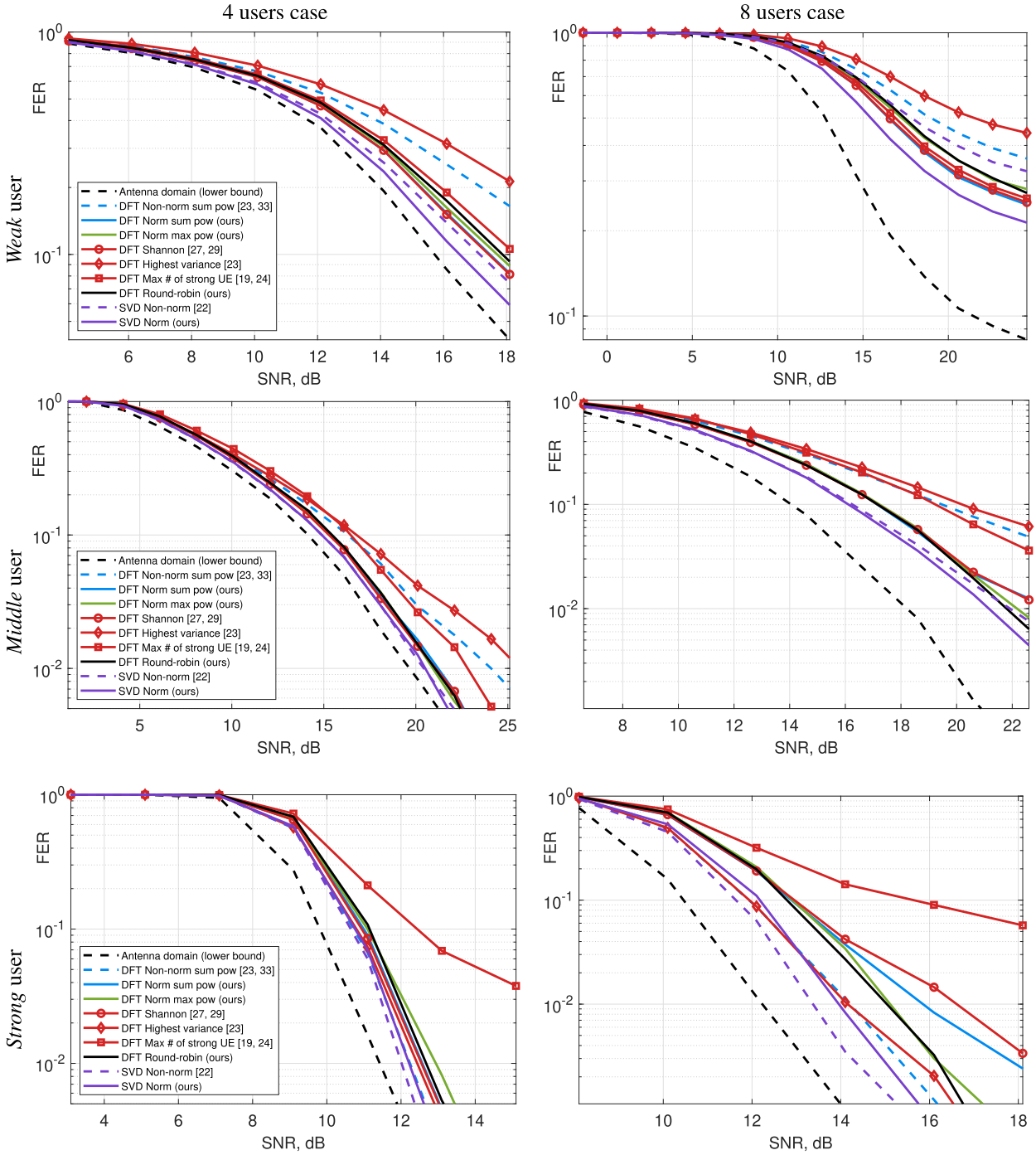

FIGURE 2. FER dependency on SNR. From left to right: 4 users case, 8 users case. From top to bottom: ***weak***, ***middle***, and ***strong*** users. Curve designations for 8 users are the same as for 4 users.

fact that in real conditions *weak* users could have significantly more degraded channels compared to *strong* users.

The methodology used in this research was designed in a way to avoid performance degradation for *weak* users and provide better system coverage without overall capacity loss. For that, we considered the link with M users having different powers on the BS side. In each experiment, the users' powers were sampled randomly from the uniform distribution $U(0dB, -20dB)$. A *strong* user always has power 0dB and *weak* and *middle* users are determined after the sampling and have different powers in different experiments. Then, the AWGN is applied with predefined power, and FER is computed for each user separately. After that, we averaged the obtained FER across all experiments for the given noise power, but not across users, to be able to independently analyze FER dependency on SNR for each particular user.

TABLE 3. SNR for FER 10^{-1} in case of different MBSS algorithms.

Algorithm	SNR for FER 10^{-1}, dB (4 UE case)			SNR for FER 10^{-1}, dB (8 UE case)		
	weak UE	*middle* UE	*strong* UE	*weak* UE	*middle* UE	*strong* UE
Antenna domain (lower bound)	15.7	14.1	9.8	21.4	14.0	10.5
DFT Non-norm sum pow [23, 33]	>25	16.3	**10.7**	>60	19.5	**11.9**
DFT Norm sum pow (proposed)	**17.4**	**15.3**	11.0	>50	**17.1**	12.9
DFT Norm max pow (proposed)	17.7	**15.4**	11.1	>55	**17.2**	12.9
DFT Shannon [27, 29]	**17.4**	**15.2**	**10.9**	**>50**	**17.2**	13.0
DFT Highest variance [23]	>25	16.8	**10.8**	>70	20.2	**11.9**
DFT Max # of strong UE [19, 24]	18.3	16.4	12.4	**>50**	19.2	15.7
DFT Round-robin (proposed)	17.9	**15.4**	11.2	>55	**17.1**	12.8
SVD Non-norm [22]	17.1	**14.9**	**10.6**	>60	16.3	**11.6**
SVD Norm (proposed)	**16.5**	**14.9**	**10.8**	**>45**	**16.1**	12.2

By measuring the dependency of FER on different SNR levels for each user, we could judge the link performance.

This approach allows us to simulate real situations with differences in UE's powers at the BS side and investigate how certain MBSS techniques affect the regular users (*middle* and *strong* ones) and the deprived users (*weak* ones). Thus, using the proposed methodology, it is possible to find an MBSS algorithm that provides high enough throughput for regular users and, at the same time, does not significantly deprive *weak* ones.

VI. SIMULATION RESULTS

In this section, the obtained results are presented and analyzed. Figure 2 represents FER dependency on SNR for *weak*, *middle*, and *strong* users in case of $M = 4$, $M = 8$ respectively. The curve labeled as **Antenna domain** corresponds to the case when no beamspace transformation was used and no signal power was lost. In this case, CE via DMRS pilots and MIMO detection were performed in the conventional antenna domain. Thus, the **Antenna domain** is the baseline since it defines the lower bound of FER which could be achieved by any beamspace selection algorithm as discussed in Section V-A. The closer FER dependency on SNR for a given beamspace selection algorithm to the **Antenna domain** curve is, the better performance the given algorithm has. In addition, the required SNR for each considered MBSS algorithm to achieve FER 10^{-1} is represented in Table 3 for convenience.

From the obtained results, we can make the following observations. First, normalization significantly improves link performance: for DFT-based sum power maximization, DFT-based max power maximization, and SVD-based selection in cases of 8 and 4 users. Second, the behavior of **DFT Shannon**, **DFT Round-robin**, **DFT Norm max pow**, and **DFT Norm sum pow** is very similar. However, the first one is more *hardware-demanding* due to an iterative selection of beams as analyzed in Section IV.

The most important finding is that our algorithms outperform approaches presented in the literature, such as **DFT Non-norm sum pow**, **DFT Shannon**, **DFT Highest variance**, and **DFT Max number of strong UE**. Moreover, we noticed that the behavior of **DFT Highest variance** is close to **DFT Non-norm sum pow** one. Thus, the most effective DFT-based algorithms are **DFT Norm max power** and **DFT Norm sum pow**.

The most accurate MBSS algorithm is the **SVD Norm** since it is closer to the **Antenna domain** curve in all considered cases. However, SVD-based algorithms are much more complex in terms of OFDM symbols transformation to the beamspace domain compared to DFT-based approaches, as shown in Section IV.

VII. CONCLUSION

In this paper, we tested several multi-user beamspace selection algorithms in a realistic propagation channel. Thus, some existing DFT-based algorithms (e.g. **DFT Highest variance** [23])) result in low system coverage since a significant performance loss was achieved for *weak* users. On the other hand, algorithm **DFT Max # of strong UE** [19], [24] can guarantee adoptable coverage at cost of significant capacity loss as it degrades the performance of *strong* users. Other DFT-based algorithms, like **DFT Shannon**, demonstrate appropriate performance and ensure low complexity of signal transformation from the antenna to the beamspace domain, but the complexity of the beamspace selection algorithm is too high. SVD-based algorithms, especially **SVD Norm**, show the best performance, but the complexity of antenna transformation to the beamspace domain is too high compared to the FFT-based transformation complexity.

To overcome the above problems, we proposed new DFT-based multi-user beamspace selection algorithms to increase system coverage without substantial overall capacity loss. The designed methodology for algorithms comparison is based on fair resource sharing in the spatial domain. Accordingly, **DFT Norm Sum power** and **DFT Norm Max power** are the best choices in terms of performance in $\mathcal{O}(N \log N)$ transformation complexity.

ACKNOWLEDGMENT

The authors acknowledge the use of computational cluster Zhores [52] for obtaining the results presented in this article. They would like to thank Skoltech, where the research was carried out.

REFERENCES

[1] B. Raaf, W. Zirwas, K.-J. Friederichs, E. Tiirola, M. Laitila, P. Marsch, and R. Wichman, "Vision for beyond 4G broadband radio systems," in *Proc. IEEE 22nd Int. Symp. Pers., Indoor Mobile Radio Commun.*, Sep. 2011, pp. 2369–2373.

[2] M. Shafi, A. F. Molisch, P. J. Smith, T. Haustein, P. Zhu, P. De Silva, F. Tufvesson, A. Benjebbour, and G. Wunder, "5G: A tutorial overview of standards, trials, challenges, deployment, and practice," *IEEE J. Sel. Areas Commun.*, vol. 35, no. 6, pp. 1201–1221, Jun. 2017.

[3] E. Hossain and M. Hasan, "5G cellular: Key enabling technologies and research challenges," *IEEE Instrum. Meas. Mag.*, vol. 18, no. 3, pp. 11–21, Jun. 2015.

[4] F. Rusek, D. Persson, B. K. Lau, E. G. Larsson, T. L. Marzetta, O. Edfors, and F. Tufvesson, "Scaling up MIMO: Opportunities and challenges with very large arrays," *IEEE Signal Process. Mag.*, vol. 30, no. 1, pp. 40–60, Jan. 2012.

[5] L. Lu, G. Y. Li, A. L. Swindlehurst, A. Ashikhmin, and R. Zhang, "An overview of massive MIMO: Benefits and challenges," *IEEE J. Sel. Topics Signal Process.*, vol. 8, no. 5, pp. 742–758, Oct. 2014.

[6] J. Jose, A. Ashikhmin, T. L. Marzetta, and S. Vishwanath, "Pilot contamination and precoding in multi-cell TDD systems," *IEEE Trans. Wireless Commun.*, vol. 10, no. 8, pp. 2640–2651, Aug. 2011.

[7] R. Bychkov, A. Osinsky, A. Ivanov, and D. Yarotsky, "Data-driven beams selection for beamspace channel estimation in massive MIMO," in *Proc. IEEE 93rd Veh. Technol. Conf. (VTC-Spring)*, Apr. 2021, pp. 1–5.

[8] G. Kalfas, M. Agus, A. Pagano, L. A. Neto, A. Mesodiakaki, C. Vagionas, J. Vardakas, E. Datsika, C. Verikoukis, and N. Pleros, "Converged analog fiber-wireless point-to-multipoint architecture for eCPRI 5G fronthaul networks," in *Proc. IEEE Global Commun. Conf. (GLOBECOM)*, Dec. 2019, pp. 1–6.

[9] H. Xie, F. Gao, and S. Jin, "An overview of low-rank channel estimation for massive MIMO systems," *IEEE Access*, vol. 4, pp. 7313–7321, 2016.

[10] A. Osinsky, A. Ivanov, and D. Yarotsky, "Bayesian approach to channel interpolation in massive MIMO receiver," *IEEE Commun. Lett.*, vol. 24, no. 12, pp. 2751–2755, Dec. 2020.

[11] W. U. Bajwa, J. Haupt, A. M. Sayeed, and R. Nowak, "Compressed channel sensing: A new approach to estimating sparse multipath channels," *Proc. IEEE*, vol. 98, no. 6, pp. 1058–1076, Jun. 2010.

[12] S. Shahbazpanahi, A. B. Gershman, and G. B. Giannakis, "Semiblind multiuser MIMO channel estimation using Capon and MUSIC techniques," *IEEE Trans. Signal Process.*, vol. 54, no. 9, pp. 3581–3591, Sep. 2006.

[13] V. Molodtsov, A. Kureev, and E. Khorov, "Experimental study of smoothing modifications of the MUSIC algorithm for direction of arrival estimation in indoor environments," *IEEE Access*, vol. 9, pp. 153767–153774, 2021.

[14] S. L. H. Nguyen and A. Ghrayeb, "Compressive sensing-based channel estimation for massive multiuser MIMO systems," in *Proc. IEEE Wireless Commun. Netw. Conf. (WCNC)*, Apr. 2013, pp. 2890–2895.

[15] H. Yin, D. Gesbert, M. Filippou, and Y. Liu, "A coordinated approach to channel estimation in large-scale multiple-antenna systems," *IEEE J. Sel. Areas Commun.*, vol. 31, no. 2, pp. 264–273, Jan. 2013.

[16] A. Adhikary, J. Nam, J.-Y. Ahn, and G. Caire, "Joint spatial division and multiplexing—The large-scale array regime," *IEEE Trans. Inf. Theory*, vol. 59, no. 10, pp. 6441–6463, Oct. 2013.

[17] A. M. Sayeed, "Deconstructing multiantenna fading channels," *IEEE Trans. Signal Process.*, vol. 50, no. 10, pp. 2563–2579, Mar. 2002.

[18] C.-K. Wen, S. Jin, K.-K. Wong, J.-C. Chen, and P. Ting, "Channel estimation for massive MIMO using Gaussian-mixture Bayesian learning," *IEEE Trans. Wireless Commun.*, vol. 14, no. 3, pp. 1356–1368, Mar. 2015.

[19] M. Mahdavi, O. Edfors, V. Owall, and L. Liu, "Angular-domain massive MIMO detection: Algorithm, implementation, and design tradeoffs," *IEEE Trans. Circuits Syst. I, Reg. Papers*, vol. 67, no. 6, pp. 1948–1961, Jun. 2020.

[20] J. Shikida, K. Muraoka, and N. Ishii, "Sparse channel estimation using multiple DFT matrices for massive MIMO systems," in *Proc. IEEE 88th Veh. Technol. Conf. (VTC-Fall)*, Aug. 2018, pp. 1–5.

[21] H. Xie, F. Gao, S. Zhang, and S. Jin, "A unified transmission strategy for TDD/FDD massive MIMO systems with spatial basis expansion model," *IEEE Trans. Veh. Technol.*, vol. 66, no. 4, pp. 3170–3184, Apr. 2017.

[22] Z. Jiang, S. Zhou, and Z. Niu, "Antenna-beam spatial transformation in C-RAN with large antenna arrays," in *Proc. IEEE Int. Conf. Commun. Workshops (ICC Workshops)*, May 2017, pp. 1215–1220.

[23] M. Mahdavi, O. Edfors, V. Owall, and L. Liu, "A low complexity massive MIMO detection scheme using angular-domain processing," in *Proc. IEEE Global Conf. Signal Inf. Process. (GlobalSIP)*, Nov. 2018, pp. 181–185.

[24] M. Mahdavi, O. Edfors, V. Owall, and L. Liu, "A VLSI implementation of angular-domain massive MIMO detection," in *Proc. IEEE Int. Symp. Circuits Syst. (ISCAS)*, May 2019, pp. 1–5.

[25] A. Hegde and K. V. Srinivas, "Matching theoretic beam selection in millimeter-wave multi-user MIMO systems," *IEEE Access*, vol. 7, pp. 25163–25170, 2019.

[26] A. M. Sayeed, J. H. Brady, F. Luo, and J. Zhang, "Millimeter-wave MIMO transceivers: Theory, design and implementation," in *Signal Processing for 5G: Algorithms and Implementations*. Hoboken, NJ, USA: Wiley, 2016.

[27] R. Pal, K. V. Srinivas, and A. K. Chaitanya, "A beam selection algorithm for millimeter-wave multi-user MIMO systems," *IEEE Commun. Lett.*, vol. 22, no. 4, pp. 852–855, Apr. 2018.

[28] X. Gao, L. Dai, Z. Chen, Z. Wang, and Z. Zhang, "Near-optimal beam selection for beamspace mmWave massive MIMO systems," *IEEE Commun. Lett.*, vol. 20, no. 5, pp. 1054–1057, May 2016.

[29] P. V. Amadori and C. Masouros, "Low RF-complexity millimeter-wave beamspace-MIMO systems by beam selection," *IEEE Trans. Commun.*, vol. 63, no. 6, pp. 2212–2223, Jun. 2015.

[30] R. Pal, A. K. Chaitanya, and K. V. Srinivas, "Low-complexity beam selection algorithms for millimeter wave beamspace MIMO systems," *IEEE Commun. Lett.*, vol. 23, no. 4, pp. 768–771, Apr. 2019.

[31] X. Gao, F. Tufvesson, O. Edfors, and F. Rusek, "Measured propagation characteristics for very-large MIMO at 2.6 GHz," in *Proc. 46th Asilomar Conf. Signals, Syst. Comput. (ASILOMAR)*, Nov. 2012, pp. 295–299.

[32] X. Gao, O. Edfors, F. Rusek, and F. Tufvesson, "Massive MIMO performance evaluation based on measured propagation data," *IEEE Trans. Wireless Commun.*, vol. 14, no. 7, pp. 3899–3911, Jul. 2015.

[33] T. Takahashi, A. Tolli, S. Ibi, and S. Sampei, "Low-complexity large MIMO detection via layered belief propagation in beam domain," *IEEE Trans. Wireless Commun.*, vol. 21, no. 1, pp. 234–249, Jan. 2022.

[34] M. A. Ruder, U. L. Dang, and W. H. Gerstacker, "User pairing for multiuser SC-FDMA transmission over virtual MIMO ISI channels," in *Proc. IEEE Global Telecommun. Conf. (GLOBECOM)*, Nov. 2009, pp. 1–7.

[35] M. A. Ruder, D. Ding, U. L. Dang, and W. H. Gerstacker, "Combined user pairing and spectrum allocation for multiuser SC-FDMA transmission," in *Proc. IEEE Int. Conf. Commun. (ICC)*, Jun. 2011, pp. 1–6.

[36] N. Prasad, H. Zhang, H. Zhu, and S. Rangarajan, "Multi-user MIMO scheduling in the fourth generation cellular uplink," *IEEE Trans. Wireless Commun.*, vol. 12, no. 9, pp. 4272–4285, Sep. 2013.

[37] A. Ivanov, A. Osinsky, D. Lakontsev, and D. Yarotsky, "High performance interference suppression in multi-user massive MIMO detector," in *Proc. IEEE 91st Veh. Technol. Conf. (VTC-Spring)*, May 2020, pp. 1–5.

[38] R. Ratasuk and A. Ghosh, "System performance of uplink multi-user MIMO in LTE," in *Proc. IEEE Veh. Technol. Conf. (VTC Fall)*, Sep. 2011, pp. 1–5.

[39] Y. Gao, B. Xia, K. Xiao, Z. Chen, X. Li, and S. Zhang, "Theoretical analysis of the dynamic decode ordering SIC receiver for uplink NOMA systems," *IEEE Commun. Lett.*, vol. 21, no. 10, pp. 2246–2249, Oct. 2017.

[40] A. Ivanov, D. Yarotsky, M. Stoliarenko, and A. Frolov, "Smart sorting in massive MIMO detection," in *Proc. 14th Int. Conf. Wireless Mobile Comput., Netw. Commun. (WiMob)*, Oct. 2018, pp. 1–6.

[41] A. Ivanov, A. Savinov, and D. Yarotsky, "Iterative nonlinear detection and decoding in multi-user massive MIMO," in *Proc. 15th Int. Wireless Commun. Mobile Comput. Conf. (IWCMC)*, Jun. 2019, pp. 573–578.

[42] S. Jaeckel, L. Raschkowski, K. Borner, and L. Thiele, "QuaDRiGa: A 3-D multi-cell channel model with time evolution for enabling virtual field trials," *IEEE Trans. Antennas Propag.*, vol. 62, no. 6, pp. 3242–3256, Jun. 2014.

[43] A. Osinsky, A. Ivanov, D. Lakontsev, R. Bychkov, and D. Yarotsky, "Data-aided LS channel estimation in massive MIMO turbo-receiver," in *Proc. IEEE 91st Veh. Technol. Conf. (VTC-Spring)*, May 2020, pp. 1–5.

[44] T. H. Nguyen, T. V. Chien, H. Q. Ngo, X. N. Tran, and E. Bjornson, "Pilot assignment for joint uplink-downlink spectral efficiency enhancement in massive MIMO systems with spatial correlation," *IEEE Trans. Veh. Technol.*, vol. 70, no. 8, pp. 8292–8297, Aug. 2021.

[45] A. Osinsky, R. Bychkov, A. Ivanov, and D. Yarotsky, "Adaptive channel interpolation in high-speed massive MIMO," in *Proc. IEEE 93rd Veh. Technol. Conf. (VTC-Spring)*, Apr. 2021, pp. 1–5.

[46] A. Osinsky, A. Ivanov, and D. Yarotsky, "Theoretical performance bound of uplink channel estimation accuracy in massive MIMO," in *Proc. IEEE Int. Conf. Acoust., Speech Signal Process. (ICASSP)*, May 2020, pp. 4925–4929.
[47] M. Rupp, C. Mehlfuhrer, and S. Caban, "On achieving the Shannon bound in cellular systems," in *Proc. 20th Int. Conf. Radioelektronika*, Apr. 2010, pp. 1–5.
[48] F. Notarnicola, "Matrix recursive expressions of the DFT of even and odd complex sequences," *Numer. Linear Algebra Appl.*, vol. 12, no. 8, pp. 793–808, 2005.
[49] A. Osinsky, A. Ivanov, and D. Yarotsky, "Efficient performance bound for channel estimation in massive MIMO receiver," *IEEE Trans. Wireless Commun.*, vol. 20, no. 11, pp. 7001–7010, Nov. 2021.
[50] A. Osinsky, A. Ivanov, and D. Yarotsky, "Spatial denoising for sparse channel estimation in coherent massive MIMO," in *Proc. IEEE 94th Veh. Technol. Conf. (VTC-Fall)*, Sep. 2021, pp. 1–5.
[51] A. Osinsky, A. Ivanov, D. Lakontsev, and D. Yarotsky, "Lower performance bound for beamspace channel estimation in massive MIMO," *IEEE Wireless Commun. Lett.*, vol. 10, no. 2, pp. 311–314, Feb. 2021.
[52] I. Zacharov, R. Arslanov, M. Gunin, D. Stefonishin, A. Bykov, S. Pavlov, O. Panarin, A. Maliutin, S. Rykovanov, and M. Fedorov, "'Zhores'—Petaflops supercomputer for data-driven modeling, machine learning and artificial intelligence installed in Skolkovo institute of science and technology," *Open Eng.*, vol. 9, no. 1, pp. 512–520, Oct. 2019.

VLADISLAV MOLODTSOV received the B.Sc. degree in applied mathematics and physics from the Moscow Institute of Physics and Technology, in 2021. He is currently pursuing the M.Sc. degree in computer science with the Skolkovo Institute of Science and Technology (Skoltech). His research interests include wireless technologies, digital signal processing, and SDR prototyping.

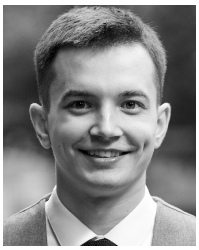

ROMAN BYCHKOV received the M.Sc. degree in applied mathematics and physics from the Moscow Institute of Physics and Technology, Moscow, in 2020. He is currently pursuing the Ph.D. degree with the Artificial Intelligence Technology Center, Skolkovo Institute of Science and Technology (Skoltech). His research interests include machine learning, digital signal processing, and wireless technologies.

ALEXANDER OSINSKY received the B.Sc. degree in applied mathematics, the M.Sc. degree in applied mathematics and physics from the Moscow Institute of Physics and Technology (MIPT), Moscow, Russia, in 2016 and 2018, respectively, and the Ph.D. degree in mathematical modeling, numerical methods and software from the Skolkovo Institute of Science and Technology (Skoltech), Moscow, in 2022.

In 2018, he was a Junior Research Scientist at the Marchuk Institute of Numerical Mathematics, Russian Academy of Sciences. Since 2019, he has been with Skoltech. His research interest includes development of numerical algorithms for problems related to linear algebra. He received the Gold Medal of the Russian Academy of Sciences for the best student work in mathematics, in 2018.

DMITRY YAROTSKY received the graduate degree from the Department of Mechanics and Mathematics, Moscow State University, in 1998, where he received the C.Sc. degree, in 2002, and the D.Sc. degree from the Institute for Information Transmission Problems (IITP), in 2015. He worked at IITP, the Dublin Institute for Advanced Studies, and Munich University. He is currently an Associate Professor and the Head of the Laboratory of Mathematical Foundations of Artificial Intelligence, Skolkovo Institute of Science and Technology (Skoltech). His interests include applied mathematics, data analysis, and optimization.

ANDREY IVANOV received the M.Sc. and Ph.D. degrees in computer science from Bauman Moscow State Technical University, Russia. He was a Researcher at industrial companies (Unique IC, Delta, Huawei, Yaliny, Impedans) in Russia, China, and Ireland. He is currently a Senior Research Scientist with the Center of Excellence in WT and IoT Technologies, Skolkovo Institute of Science and Technology (Skoltech). His research interests include digital signal processing, wireless communications, and MIMO technologies.